JOURNAL OF SOLID STATE CHEMISTRY **102,** 267–276 (1993)

Combustion Route to Fine Particle Perovskite Oxides

S. SUNDAR MANOHARAN AND K. C. PATIL

Department of Inorganic and Physical Chemistry, Indian Institute of Science, Bangalore 560 012, India

Received December 17, 1991, in revised form June 2, 1992; accepted June 3, 1992

Fine particle perovskite oxides such as $LnCrO_3$ (where Ln = La, Pr, Nd, Sm, Dy, Gd, and Y), $La_{1-x}Sr_xMnO_3$ (x = 0.0 to 0.5), $LaCoO_3$, and $LaNiO_3$ have been prepared by the combustion of corresponding metal nitrate–tetraformal trisazine (TFTA) mixtures at 350°C/500°C in a few minutes under ambient conditions. The oxides are of submicrometer size with specific surface area ranging from 3–20 m^2/g. The oxides have been characterized further by TEM and SEM studies. Sintering of $LaCrO_3$ at 1500°C for 2 hr resulted in 85% (5.2 g/cm^3) of the theoretical density.

1. Introduction

Perovskite and related oxides have attracted much attention in recent years; their magnetic, structural, refractory, and catalytic properties have been extensively investigated (*1*, *2*). Materials with high electrical conductivity which can be used in corrosive environments as well as at elevated temperatures have been in great demand. Because of their high melting point and high electronic conductivity, rare earth chromites have been quite attractive for such applications (*3*). One of the promising materials is $LaCrO_3$, which satisfies many of the high-temperature electrode requirements for magnetohydrodynamic (MHD) power generators and solid oxide fuel cells (SOFC) (*4*). Lanthanum manganite, $LaMnO_3$ has been studied extensively due to its potential application as an air electrode in SOFC (*5*). Strontium-substituted $LaMnO_3$ has received attention as a catalyst for the oxidation of CO, for the control of automobile emissions (*6*). Lanthanum cobaltite, $LaCoO_3$, and $LaNiO_3$ have recieved prime importance due to their electrical properties (*7*, *8*).

Recently there has been a new trend in the ceramic community toward novel chemical routes of synthesis (*9*) which can lead to ultrafine, high-surface-area powders. Such processes involve forming of intermediate organometallic materials followed by calcination and sintering to get high-density ceramics. Precursors such as carbonates (*10*), hydroxides (*11*), oxalates (*12*), and complex cyanides (*13*) have been employed to prepare ternary oxides of the type $LaMO_3$ (where M = Cr, Mn, Co, and Ni). Recently Kadogawa and Kitayama (*14*) have employed a sol–gel technique to prepare $LaCrO_3$ which involves mixing of corresponding metal nitrates with a small amount of $Si(OC_2H_5)_4$ as the hydrolyzing agent and alkaline metal chloride as a mineralizer. Yoshimura *et al.* (*15*) prepared $LaCrO_3$ under hydrothermal condition at 400°C and 100

0022-4596/93 $5.00

MPa using $Cr(OH)_3$ and La_2O_3. In order to fabricate a porous air electrode, Lessing (*16*) has employed polymeric precursors to prepare $La(Sr)MnO_3$ of desired particle morhology. In all these wet chemical methods, the emphasis is to prepare oxides with precise control of the stoichiometry and homogeneity.

Self-propagating high-temperature synthesis (SHS), developed by Merzanova and Borovinskaya (*17*), has been used to prepare nonoxide materials such as carbides, borides, nitrides, and silicides. A historical perspective of SHS has been reviewed recently (*18–20*). Synthesis of sulphides, nitrides, silicides, and GaAs has been reported (*21*) recently by a metathetical (exchange) pathway. These processes have disadvantages such as acquiring finely divided starting elements, incomplete conversion to products, and the need for further processing. A modified combustion process (which uses solution precursors) developed in our laboratory has been successfully used to prepare fine particle aluminas (*22, 23*), chromites (*24–26*), ferrites (*27*), titanates (*28*), as well as high-T_c cuprates (*29, 30*). We now report the preparation of a number of perovskite oxides by this novel combustion method in a few minutes. The oxides prepared include $LnCrO_3$ (where Ln = La, Pr, Nd, Sm, Gd, Dy, and Y), $LaMO_3$ (where M = Mn, Co, and Ni), as well as $La(Sr)MnO_3$. The products have been characterized by XRD, particle size analysis, surface area measurement, SEM, and TEM techniques.

2. Experimental

The stoichiometric composition of the metal nitrate–TFTA mixtures were calculated based on the total oxidizing and reducing valencies of the oxidizer and fuel which serve as numerical coefficients for stoichiometric balance so that the equivalence ratio Φ_e is unity, i.e., O/F = 1.0, and the energy released is at maximum (*31*). According to the concepts employed in propellant chemistry (*31*) the elements C, La, Sr, Mn, H, or any other metal are considered as reducing species with the corresponding valencies +4, +3, +2, +2, +1 (or valency of the metal ion in that compound), respectively. The element oxygen is considered as the oxidizing species with valency −2. The valency of nitrogen is considered to be zero. Accordingly, the oxidizing and reducing valencies of the compounds used in the combustion mixtures can be calculated. For divalent and trivalent metals the ratio of metal nitrate to TFTA will be 1 : 0.3571 and 1 : 0.5357 moles, respectively. The preparation of $LaCrO_3$, $LaMnO_3$, and $LaCoO_3$ is described below as representative.

2.1. Preparation of TFTA

Tetraformal trisazine, TFTA ($C_4H_{16}N_6O_2$), was prepared by the reaction of formaldehyde (150 ml, 4 mole) and hydrazine hydrate (76 ml of 99% $N_2H_4 \cdot H_2O$, 3 mole) at 0°C with constant stirring (*24*).

2.2. Combustion Synthesis of Lanthanum Chromite, $LaCrO_3$

Lanthanum nitrate (5.4127 g), chromium nitrate (5.0018 g), and TFTA (2.4135 g) were dissolved in a minimum quantity of water in a 300-cm^3 pyrex dish. The dish containing the mixture was heated in a muffle furnace maintained at 500°C. The solution boils and undergoes dehydration, followed by exothermic decomposition (with an *in situ* flame temperature of 1100 ± 100°C) to yield a solid oxide product. The product is fine, foamy, and voluminous. All other rare earth chromites, $LnCrO_3$, where Ln = Pr, Nd, Sm, Gd, Dy, and Y, were prepared in a similar way.

2.3. Combustion Synthesis of Lanthanum Manganite, $LaMnO_3$

$La(NO_3)_3 \cdot 9H_2O$ (11.2132 g) and $Mn(NO_3)_2 \cdot 4H_2O$ (6.500 g) and TFTA

(6.9258 g) were dissolved in a minimum amount of water in a dish of 300 cm^3 capacity. The dish containing the redox mixture was introduced into a muffle furnace maintained at 500°C. The solution initially boils with frothing and foaming to the capacity of the container. At the point of complete dehydration, the surface of the foam ignites with an appearance of a flame (1100 ± 100°C) which propagates to the bottom of the container to convert the whole mixture to a solid oxide product. The combustion residue is foamy and black in color. The whole reaction is over within 5 min. Strontium-substituted rare earth manganites were prepared in a similar way by the addition of required amount of strontium nitrate to the redox mixture. The amount of Mn^{3+} and Mn^{4+} in the Sr^{2+}-doped $LaMnO_3$ was determined by the sodium bismuthate method (*32*).

2.4. Combustion Synthesis of Lanthanum Cobaltite, $LaCoO_3$

$La(NO_3)_2 \cdot 9H_2O$ (3.422 g), $Co(NO_3)_2 \cdot 6H_2O$ (2.3 g), and TFTA (2.8484 g) were dissolved in a minimum amount of water in a 1-liter beaker and heated over a hot plate maintained at 350°C. The mixture boils and ignites to give a black, X-ray amorphous powder, which on further heating at 800°C for 1 hr resulted in a crystalline single phase $LaCoO_3$ as identified by powder XRD.

Precaution: The combustion synthesis is safe as long as the reaction is carried out in an open vessel and in gram quantities.

2.5. Physical Methods

The combustion derived perovskite oxides were charactcrized using Philips powder X-ray diffractometer model PW 1050/70 using CuK_α radiation with a nickel filter. The powder densities of the as-prepared oxides were measured using a pycnometer in a xylene medium. The surface area measurements were made by nitrogen adsorption employing a Micromeritics Accusorb 2100 E instrument. Particle size analysis was done using a Micron photosizer Model SKC 2000 based on the light scattering principle employing the sedimentation technique. The morphology of the powders was studied using a Philips EM 301 transmission electron microscope (TEM) operated at 100 kV. The microstructure of the sintered compact was studied by Cambridge Stereoscan Model S-150 scanning electron microscope (SEM). The flame temperature was measured using an optical pyrometer.

3. Results and Discussion

The metal nitrate–TFTA mixture when heated rapidly at 350°C/500°C ignites and burns with a flame (Temp. > 1000°C). The retention time of the flame is less than a minute, and as the reaction is adiabatic in nature, the heat evolved is used for the formation of the oxide product and does not affect the pyrex vessel.

Tetraformal trisazine (TFTA) is reported (*33*) to be hypergolic with red fuming nitric acid (RFNA). Azines having N–N bonds are energetic fuels and undergo highly exothermic reactions on combustion. Pyrolysis, mass spectral studies (*34*) of TFTA show that the major gaseous products are HNCO and NH_3. The chemical reaction between the gaseous decomposition products of TFTA ($HNCO,NH_3$) and metal nitrates (oxides of nitrogen) is highly exothermic, which helps the instantaneous formation of perovskite oxides. The combustion of TFTA also results in the evolution many gases such as H_2O, CO_2, N_2, etc., which produce fine particle oxides.

3.1. Properties of $LnCrO_3$

Actual weights of metal nitrate and TFTA used for the combustion and some properties of the chromites are listed in Table I. The formation of single phase $LnCrO_3$ was

TABLE I

SOME PROPERTIES OF RARE EARTH ORTHOCHROMITES

Stoichiometric composition	Product	Density (g/cm^3)	Surface area (m^2/g)	Particle Size (μm)	
				Surface area	Sedimentation technique
5.4127 g $La(NO_3)_3 \cdot 9H_2O$ + *B* + *C*	$LaCrO_3$	3.61	8.7	0.19	2.8
6.111 g $Pr(NO_3)_3 \cdot 9H_2O$ + *B* + *C*	$PrCrO_3$	4.5	6.9	0.19	1.8
5.479 g $Nd(NO_3)_3 \cdot 9H_2O$ + *B* + *C*	$NdCrO_3$	4.8	8.0	0.15	0.95
5.555 g $Sm(NO_3)_3 \cdot 9H_2O$ + *B* + *C*	$SmCrO_3$	4.63	11.8	0.1	3.6
5.642 g $Gd(NO_3)_3 \cdot 9H_2O$ + *B* + *C*	$GdCrO_3$	4.8	15.5	0.08	3.0
5.482 g $Dy(NO_3)_3 \cdot 9H_2O$ + *B* + *C*	$DyCrO_3$	4.7	6.6	0.19	2.5
4.787 g $Y(NO_3)_3 \cdot 9H_2O$ + *B* + *C*	$YCrO_3$	4.0	16.85	0.08	1.9

Note. *B* = 5.0018 g $Cr(NO_3)_3 \cdot 9H_2O$; *C* = 2.4135 g Tetraformal trisazine.

confirmed by their characteristic X-ray powder diffraction patterns. A typical X-ray pattern of the as-prepared $LaCrO_3$ is shown in Fig. 1a. The lattice constants (a = 5.471 Å, b = 5.502 Å, c = 7.751 Å) calculated from the XRD pattern agree well with the literature values (*35*), corresponding to the orthorhombic symmetry. The average crystallite size calculated from X-ray line broadening using the Scherrer equation (*36*) is 40

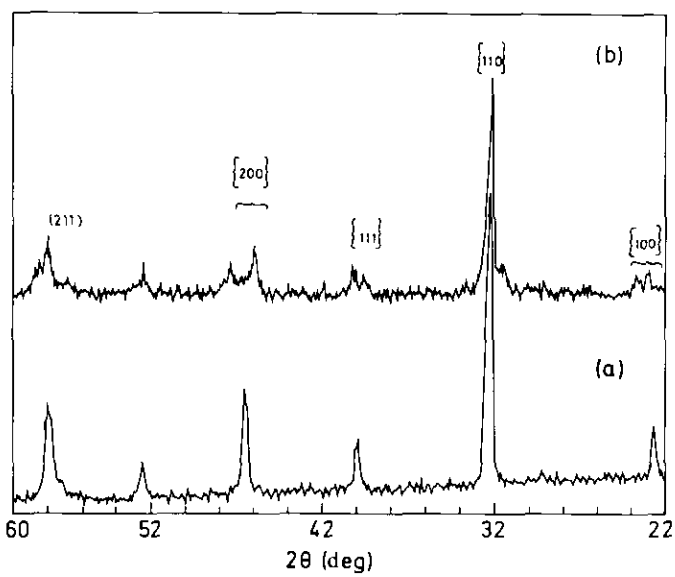

FIG. 1. Powder X-ray diffraction pattern of as-prepared (a) $LaCrO_3$ and (b) $LaMnO_3$.

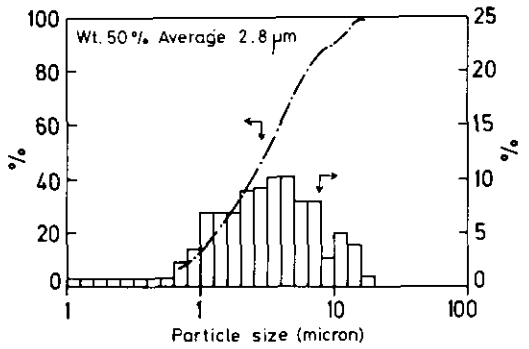

FIG. 2. Particle size distribution curve of $LaCrO_3$.

nm. The fine particulate characteristics are further evident from the density, particle size and surface area values (Table I). The BET specific surface area of the orthochromites obtained ranges from 6–17 m^2/g, $YCrO_3$ having the largest surface area. This value is significantly higher than for $LnCrO_3$ prepared by the conventional ceramic method (< 4 m^2/g) (*37*). The specific surface area of the orthochromites reported by the citrate method is 5 m^2/g, even though the formation temperature is moderately lower (750°C/4 hr) than that for the ceramic technique. The higher surface area of $LaCrO_3$ obtained by the combustion process may be attributed to the evolution of cold gases such as H_2O, N_2, and CO_2 which appear to dissipate the heat and inhibit the powder from sintering. The combustion-derived $LnCrO_3$ are fine and voluminous in nature. For example, the tap density of $LaCrO_3$ is 0.06 g/cm^3. The powder density value corresponds to 50–55% of the theoretical density. A particle size distribution curve of $LaCrO_3$ is shown in Fig. 2. The average agglomerate size as measured by the sedimentation technique for rare earth chromites is 1–4 μm. The histogram (Fig. 2) reveals the narrow particle size distribution of the combustion-derived $LaCrO_3$.

The morphology of the particles is shown in the TEM micrograph (Fig. 3a). The combustion process yields nearly spherical particles with a considerable degree of agglom-

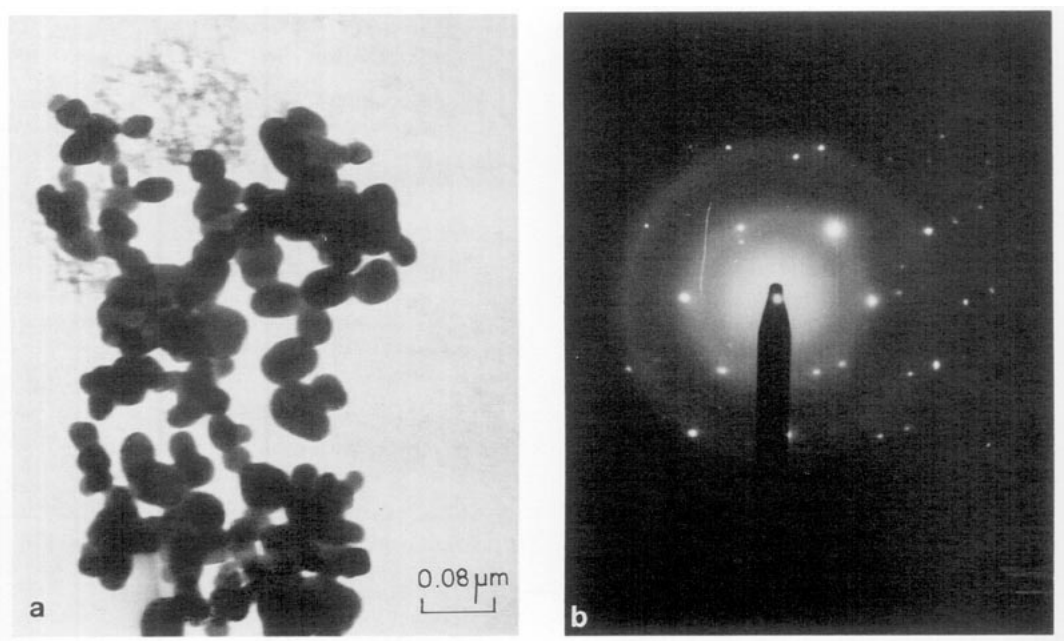

FIG. 3. TEM micrographs of as-prepared $LaCrO_3$ (a) agglomerate and (b) an electron diffraction pattern.

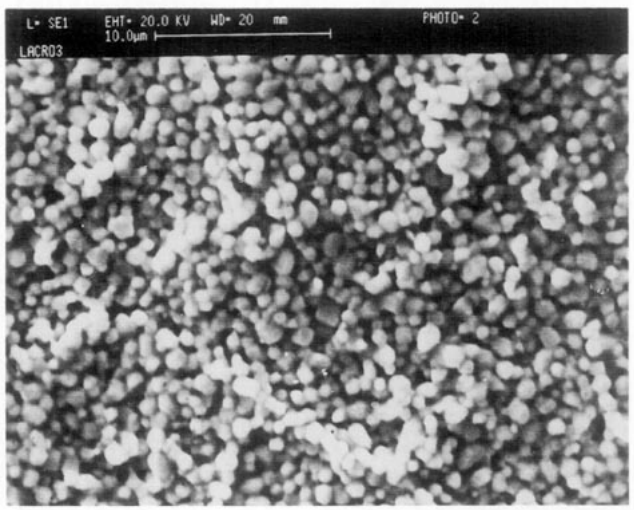

FIG. 4. SEM micrograph of $LaCrO_3$ sintered in air at 1500°C for 2 hr.

eration. The extent of agglomeration could be attributed to the fineness of the particles. Figure 3b shows the electron diffraction pattern of $LaCrO_3$, indicating that they are highly crystalline in nature. The electronic spectrum of $LaCrO_3$ solid in nujol mull shows characteristic bands at 16,500 and 22,050 cm^{-1}, corresponding to $4A_{2g} \rightarrow 4T_{2g}$ and $4A_{2g} \rightarrow 4T_{1g}$ and a broad band with an inflection at 30,300 and 28,120 cm^{-1}, owing to $4A_{2g} \rightarrow 4T_{1g}$ transitions, which is in accordance with the reported values corresponding to the Cr^{3+} ion (*38*).

A sintering study of fine particle $LaCrO_3$ was carried out by compacting the powder by uniaxial pressing at 5 MPa. The cylindrical compacts (12 × 3 mm) were sintered at 1500°C for 5 hr without adding any sintering aids. An SEM micrograph of the sintered compact is shown in Fig. 4. The microstructure reveals uniform and fine grain growth, thus demonstrating that a uniform particle size provides a measure of stability against exaggerated grain growth. The sintered density is 5.2 g/cm^3, which corresponds to 85% of the theoretical value.

3.2. *Properties of* $La_{1-x}Sr_xMnO_3$

Lanthanum manganite, $LaMnO_3$, and strontium-substituted derivatives were prepared using metal nitrate–TFTA redox mixtures, at 500°C in a few minutes. Formation of a single phase product was confirmed by powder XRD. Figure 1b shows the X-ray pattern of the as-prepared $LaMnO_3$. The lattice constants calculated from XRD match well with the reported values for $LaMnO_3$(*39*); calculated values are a = 5.532 Å, b = 5.753 Å, and c = 7.713 Å, and the reported values are a = 5.535 Å, b = 5.758 Å, and c = 7.708 Å. Analytical data and some properties of $La(Sr)MnO_3$ are summarized in Table II. It may be noted that with increase in strontium content, the Mn^{4+} concentration increases steadily. The presence of Mn^{3+}/Mn^{4+} couple leads to nonstoichiometry in these oxides. The powder density values of these oxides are in the range of 55–65% of the theoretical value. The specific surface area of the oxides are in the range of 5–15 m^2/g. It is interesting to note that with an increase in strontium

TABLE II

ANALYTICAL DATA AND SOME PROPERTIES OF $La_{1-x}Sr_xMnO_3$ (WHERE x = 0.0–0.5)

x	wt% Mn(III)	wt% Mn(IV)	Total Mn% (theor. value)	Density (g/cm^3)	Surface area (m^2/g)	Particle size (μm) Surface area	Particle size (μm) Sedimentation technique
0.0	19.86	2.836	22.7 (22.71)	4.9	4.5	0.27	0.85
0.2	19.45	4.23	23.69 (23.72)	4.7	7.5	0.17	0.97
0.3	20.00	4.30	24.3 (24.25)	4.75	9.5	0.13	1.1
0.4	20.50	4.35	24.85 (24.87)	4.68	12.0	0.10	0.9
0.5	19.75	5.59	25.34 (25.4)	4.5	14.5	0.09	0.8

content there is a steady increase in specific surface area. This may be attributed to the time taken by the *in situ* temperature to persist during the combustion of the redox mixtures. It was observed that, with an increase in strontium nitrate content in the redox mixture, the *in situ* flame retention was lower compared to the unsubstituted $LaMnO_3$. As a result, $La_{0.5}Sr_{0.5}MnO_3$ has large surface area compared to $LaMnO_3$. The average agglomerate size of the oxides is in the range of 0.85–1.5 μm. The particle size (0.2 μm) as calculated from TEM micrograph (Fig. 5) shows that the particles are of uniform size and shape. The SEM micrograph of the as-prepared powder appears as shown in Fig. 6. These large, dense, sintered "chunks" are particularly useful for feeding through a plasma spray gun to form fuel-cell electrodes (*16*). Our observations are similar to those for $LaMnO_3$ prepared by the Pechini process (*16*) at 800 and 1100°C. The high temperature that is liberated *in situ* (> 1000°C) tends to make large crystallites that are very strongly agglomerated.

3.3. Properties of Lanthanum Cobaltite, $LaCoO_3$, and Lanthanum Nickelate, $LaNiO_3$

Unlike the preparation of lanthanum chromites and manganites, the stoichiometric compositions of the redox mixtures were altered to obtain $LaCoO_3$ and $LaNiO_3$. When the redox compositions dictated by the O/F ratio were taken, the reaction was found to be highly exothermic. The XRD pattern of the as-prepared powder showed a mixture of La_2CoO_4 and CoO (Fig. 7) and La_2NiO_4 and NiO. It is reported (*40–42*) that the formation of $LaCoO_3$ and $LaNiO_3$ proceeds via La_2CoO_4 and La_2NiO_4, respectively. This is because the divalent state of cobalt and nickel is more favored at low

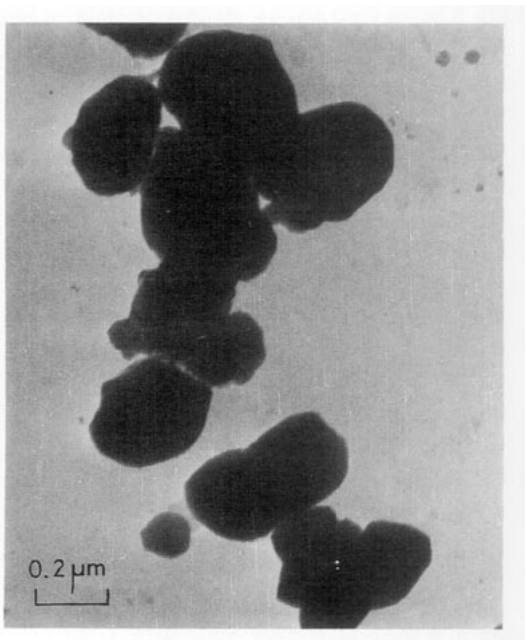

FIG. 5. TEM micrograph of as-prepared $LaMnO_3$.

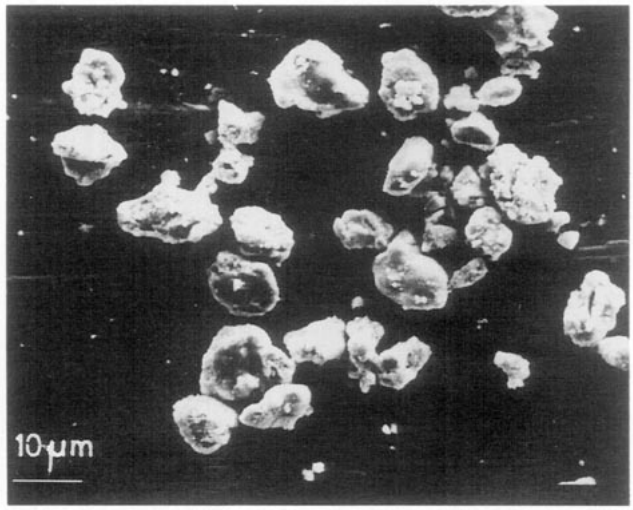

FIG. 6. SEM micrograph of as-prepared $LaMnO_3$.

temperatures and under ambient conditions. Moreover, since the K_2NiF_4 structure is stable, the combustion appears to favor La_2CoO_4 and La_2NiO_4 formation. Demazeau *et al.* (*43*) have employed a high-pressure method to convert all Ni^{2+} ions to Ni^{3+} for the formation of $LaNiO_3$. Therefore, in order to prepare $LaCoO_3$ and $LaNiO_3$, an oxidizer-rich (fuel-lean) mixture was chosen. However, on combustion of

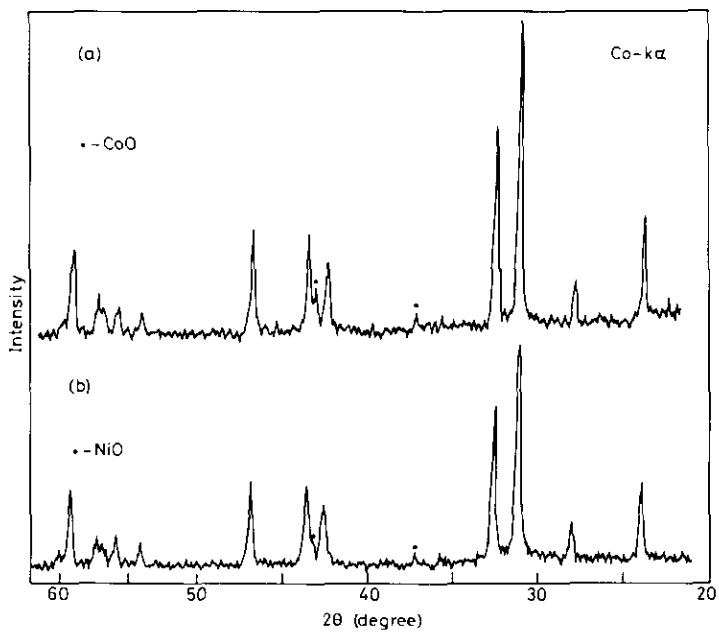

FIG. 7. X-ray powder diffraction pattern of (a) La_2CoO_4 and CoO; (b) La_2NiO_4 and NiO

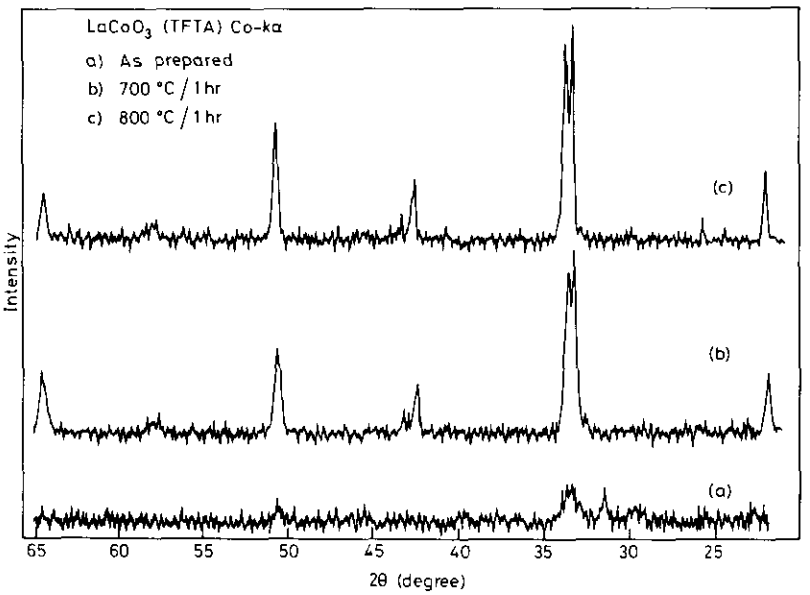

FIG. 8. X-ray diffraction pattern of $LaCoO_3$ (a) as-prepared powder at 350°C, (b) annealed at 700°C/1 hr, and (c) annealed at 800°C/1 hr.

these oxidizer-rich redox mixtures the solid oxide product obtained was found to be X-ray amorphous. The exothermicity of the combustion was found to be controlled, in contrast to the reaction with the stoichiometric (O/F = 1.0) mixtures. The amorphous powder, when heated at 800°C for 1 hr, gave a single phase XRD pattern corresponding to $LaCoO_3$ and $LaNiO_3$. Figure 8 shows the XRD pattern of $LaCoO_3$ as a function of temperature. The as-prepared powder (Fig. 8) shows a weakly crystalline pattern, which on heating for 1 hr shows single phase pattern. It is gratifying to note that the preparation of $LaCoO_3$ could be achieved in a short time (< 1 hr), which is attributed to the reactivity of the amorphous powder. The as-prepared powders are fine and voluminous in nature with a tap density of about 0.04 g/cm^3. The density of the powders calcined at 800°C are in the range of 55–60% of the theoretical value. The surface areas of calcined $LaCoO_3$ and $LaNiO_3$ are 3.5 and 4.8 m^2/g, respectively.

4. Conclusion

Fine particle perovskite oxides such as chromites, manganites, cobaltite, and nickelate have been prepared by a combustion process in a short time. The combustion process minimizes many of the processing difficulties encountered by the wet chemical methods. Effective doping of Sr ions in the $A-$site of $LaMnO_3$ has been achieved by this process.

Acknowledgment

One of the authors (SSM) thanks the Council of Scientific and Industrial Research for the award of a Senior Research Fellowship.

References

1. N. RAMDASS, *Mater. Sci. Eng.* **36,** 231 (1978).
2. S. NOMURA, *in* "Crystallographic and Magnetic Properties of Perovskite and Perovskite Related Oxides," p. 368, Springer-Verlag, Berlin (1978).
3. S. HAYASHI, K. FUKAYA, AND H. SAITO, *J. Mater. Sci.* **7,** 457 (1988).

4. W. J. Weber, C. W. Griffin, and J. L. Bates, *J. Am. Ceram. Soc.* **70**(4), 265 (1987).
5. S. Song, M. Yoshimura, and S. Somiya, *Yogyo-Kyokai-Shi* **90,** 484 (1982).
6. J. H. Kuo, H. U. Anderson, and D. M. Sparlin, *J. Solid State Chem.* **83,** 52 (1984).
7. J. L. G. Fierro, J. M. D. Tascon, and L. G. Tejuca, *J. Catal.* **89,** 209 (1984).
8. D. B. Meadowcroft, *Nature* **226,** 847 (1970).
9. D. Segal, "Chemical Synthesis of Advanced Ceramic Materials," Cambridge Univ. Press, Cambridge (1989).
10. H. S. Horowitz and J. M. Longo, *Mater. Res. Bull.* **13,** 1359 (1978).
11. K. Vidyasagar, J. Gopalakrishnan, and C. N. R. Rao, *J. Solid State Chem.* **58,** 29 (1985).
12. K. Vidyasagar, J. Gopalakrishnan, and C. N. R. Rao, *Inorg. Chem.* **23,** 1206 (1984).
13. P. K. Gallagher, *Mater. Res. Bull.* **3,** 225, (1984).
14. Y. Kadogawa and N. Kitayama, *Chem. Express* **1**(3), 145 (1986).
15. M. Yoshimura, S. Song, and S. Somiya, *Yogyo-Kyokai-Shi* **90**(2), 91 (1982).
16. P. A. Lessing, *Am. Ceram. Soc. Bull.* **68**(5), 1002 (1989).
17. A. G. Merzanova and I. P. Borovinskaya, *Dokl. Akad. Nauk. SSSR (Engl Transl.)* **204,** 429 (1972).
18. Z. A. Munir and U. Anselmi-Tamburini, *Mater. Sci. Rep.* **3,** 277 (1989).
19. H. C. Yi and J. J. Moore, *J. Mater. Sci.*, **25,** 1159 (1990).
20. V. Hlavacek, *Am. Ceram. Soc. Bull.* **70,** 240 (1991).
21. J. B. Wiley and R. B. Kaner, *Science* **255,** 1093 (1992).
22. J. J. Kingsley and K. C. Patil, *Mater. Lett.* **6,** 427 (1988).
23. J. J. Kingsley, K. Suresh, and K. C. Patil, *J. Solid State Chem.* **88,** 435 (1990).
24. S. Sundar Manoharan, N. R. S. Kumar,and K. C. Patil, *Mater. Res. Bull.* **26**(5), 731 (1991).
25. S. Sundar Manoharan and K. C. Patil, *J. Am. Ceram. Soc.* **75**(4), 1012 (1992).
26. R. Gopichandran and K. C. Patil, *Mater. Lett.* **12,** 437 (1992).
27. K. Suresh, N. R. S. Kumar, and K. C. Patil, *Adv. Mater.* **3,** 148 (1991).
28. M. Maria Amala Sekar and K. C. Patil, *J. Mater. Chem.*, **2,** 749 (1992).
29. S. Sundar Manoharan, V. Prasad, S. V. Subramanyam, and K. C. Patil, *Physica C* **190,** 225 (1992).
30. R.Gopichandran and K. C. Patil, *Mater. Res. Bull.* **27,** 147 (1992).
31. S. R. Jain, K. C. Adiga, and V. R. Pai Verneker, *Combust. Flame* **40,** 71 (1981).
32. E. Bloom, Jr. T. Y. Kometani, and J. W. Mitchell, *J. Inorg. Nucl. Chem.* **40,** 403 (1978).
33. S. R. Jain, *Combust. Flame* **28,** 101 (1977).
34. M. S. Hegde, S. Sundar Manoharan, and K. C. Patil *in* "Proc. of Eigth Natl. Symp. on Thermal Analysis, RRL, Bhubaneswar, Dec. 19–21, 1991."
35. J. M. Gonzalez-Calbet, J. Ramirez, and M. Vallet-Regi, *J. Less-Common Met.* **157,** 271 (1990).
36. H. Klug and L. Alexander, "X-ray Diffraction Procedures," p. 491, Wiley, New York (1962).
37. P. H. Courty, H. Ajot, C. H. Marcilly, and B. Demon, *Powder Technol.* **7,** 21 (1973).
38. A. Roy and K. Nag, *J. Inorg. Nucl. Chem.* **40,** 1501 (1978).
39. K. Kamata, T. Nakajima, T. Hayashi, and T. Nakamura, *Mater. Res. Bull.* **13,** 49 (1978).
40. J. L. G. Fierro, J. M. D. Tascon, and L. G. Tejuca, *J. Catal.* **93,** 83 (1985).
41. P. Odier, Y. Nigara, J. Coutures, and M. Sayer, *J. Solid State Chem.* **56**(1), 32 (1985).
42. J. Christopher, M. P. S. Kumar, and C. S. Swamy, *J. Mater. Sci.* **23,** 4263 (1988).
43. G. Demazeau, A. Marbeut, M. Pouchard, and P. Hagenmuller, *J. Solid State Chem.* **3,** 582 (1971).